Talanta 117 (2013) 45–54

Contents lists available at ScienceDirect

Talanta

journal homepage: www.elsevier.com/locate/talanta

Elaboration of ammonia gas sensors based on electrodeposited polypyrrole—Cobalt phthalocyanine hybrid films

Tilia Patois [a,b], Jean-Baptiste Sanchez [c], Franck Berger [c], Patrick Fievet [a], Olivier Segut [d], Virginie Moutarlier [a], Marcel Bouvet [e], Boris Lakard [a,*]

[a] Institut UTINAM, UMR CNRS 6213, University of Franche-Comté, 16 route de Gray, 25030 Besançon, France
[b] Institute of Condensed Matter and Nanosciences, Université Catholique de Louvain, Croix du Sud, 1/4, 1348 Louvain-la-Neuve, Belgium
[c] Laboratoire Chrono-Environnement, UMR CNRS 6249, University of Franche-Comté, 16 Route de Gray, 25030 Besançon, France
[d] Laboratoire MOLTECH-Anjou, UMR-CNRS 6200, Université d'Angers, 2 bd Lavoisier, 49045 Angers, France
[e] Institut de Chimie Moléculaire de l'Université de Bourgogne, UMR-CNRS 6302, University of Bourgogne, 9 avenue Alain Savary, 21078 Dijon, France

ARTICLE INFO

Article history:
Received 19 May 2013
Received in revised form
26 August 2013
Accepted 28 August 2013
Available online 31 August 2013

Keywords:
Gas sensors
Hybrid materials
Polypyrrole
Phthalocyanine
Electrochemistry
Ammonia

ABSTRACT

The electrochemical incorporation of a sulfonated cobalt phthalocyanine (sCoPc) in conducting polypyrrole (PPy) was done, in the presence or absence of $LiClO_4$, in order to use the resulting hybrid material for the sensing of ammonia. After electrochemical deposition, the morphological features and structural properties of polypyrrole/phthalocyanine hybrid films were investigated and compared to those of polypyrrole films. A gas sensor consisting in platinum microelectrodes arrays was fabricated using silicon microtechnologies, and the polypyrrole and polypyrrole/phthalocyanine films were electrochemically deposited on the platinum microelectrodes arrays of this gas sensor. When exposed to ammonia, polymer-based gas sensors exhibited a decrease in conductance due to the electron exchange between ammonia and sensitive polymer-based layer. The characteristics of the gas sensors (response time, response amplitude, reversibility) were studied for ammonia concentrations varying from 1 ppm to 100 ppm. Polypyrrole/phthalocyanine films exhibited a high sensitivity and low detection limit to ammonia as well as a fast and reproducible response at room temperature. The response to ammonia exposition of polypyrrole films was found to be strongly enhanced thanks to the incorporation of the phthalocyanine in the polypyrrole matrix.

1. Introduction

Since the conductive properties of oxidatively doped polyacetylenes was evidenced in the 1970s [1], π-conjugated polymers have been extensively studied. Amongst conducting polymers, polypyrrole (PPy) has been one of the most studied because of its easy deposition from aqueous and non-aqueous media using either chemical or electrochemical oxidation. Electrodeposited PPy films have already been used for many different applications. An interesting example of application concerns sensors where PPy films are used as sensitive layer. Thus, many kinds of PPy-based sensors have been developed including: pH sensors [2–5], chemical sensors for the detection of zinc ions [6], silver ions [7], copper ions [8] or nitrate ions [9], DNA biosensors [10–12] and enzymatic biosensors [13–15].

Polypyrrole has also been used as active layer for gas sensors and it has been demonstrated that polypyrrole is a promising material for this application. Indeed polypyrrole-based gas sensors are interesting for environmental pollution monitoring because, upon exposure to vapor, the polymer shows rapid conductivity changes, which are generally reversible at room temperature. These characteristics are interesting since most of the commercially-available sensors, usually based on metal oxides, work at high temperatures (300–400 °C). In particular, several authors developed polypyrrole-based ammonia gas sensors and tried to optimize the stability, sensitivity and response time of the gas sensors. These studies demonstrated the influence of electropolymerization parameters including: initial conductivity [16], doping anions [16–18], electrodeposition potential [18], pyrrole and anion concentration [18]. Other studies have tried to combine polypyrrole with another material to improve the detection abilities of the ammonia gas sensors. This is the case of Bai et al. [19] who electrochemically co-polymerized polypyrrole and sulfonated polyaniline to obtain an ammonia sensor which was efficient for concentrations higher than 20 ppm. Other authors have synthesized hybrid materials composed of polypyrrole and carbon materials such as graphite and graphite oxide [20] or single-walled carbon nanotubes [21], and also hybrid materials composed of polypyrrole and metal oxides such as ZnO [22] or TiO_2 particles [23]. Another

* Corresponding author. Tel.: +33 3 81 66 20 46.
E-mail address: boris.lakard@univ-fcomte.fr (B. Lakard).

0039-9140/$ - see front matter © 2013 Elsevier B.V. All rights reserved.
http://dx.doi.org/10.1016/j.talanta.2013.08.047

alternative consists in incorporating organic molecules into the polypyrrole matrix. Indeed, it is expected that the combination of molecular compounds and conducting polymer films creates synergetic effects between the two components. For example the preparation of hybrid materials has already been achieved by combining polypyrrole with cyclodextrines [24–26], metal porphyrins [27–29] or metal phthalocyanines [30,31]. In particular, the works from Radhakrishnan et al. [30] and from Tiwari et al. [31] have shown that it is possible to obtain a hybrid material by electrochemical polymerization from an electrolyte containing pyrrole and copper phthalocyanine. It must also be noticed that metal phthalocyanines are very interesting for applications in the field of chemical sensors since they have already been successfully used as sensitive layers of gas sensors [31–35]. Furthermore, the study from Tiwari et al. is particularly interesting since the electrosynthesized polypyrrole/copper phthalocyanine material was successfully tested as sensitive film of a gas sensor for the selective detection of a nerve gas simulant dimethyl methyl phosphonate (DMMP). In particular, the sensor was unaffected by the interfering vapors like ethanol, benzene, toluene and hexane even at high concentration, which makes it more suitable for DMMP sensing in presence of them. In a previous study we have also shown that a polypyrrole/phthalocyanine film can respond to ammonia concentration changes whatever the relative humidity rate, in contrast to traditional gas sensors based on phthalocyanines [36].

In this context, the present work aimed at electrosynthesizing hybrid materials from electrolytic aqueous solutions containing pyrrole, sulfonated copper phthalocyanine and lithium perchlorate (for only some of them). After characterization, these hybrid materials were deposited on platinum microstructured electrode arrays and tested as sensitive layers of chemiresistive gas sensors. More precisely, the conductance changes of PPy/sCoPc-based sensors were measured during their exposition to different ammonia concentrations, leading to the determination of their characteristics (response time, sensitivity, reproducibility, kinetics).

2. Experimental

2.1. Microfabrication

Silicon microtechnologies were used to fabricate microsystems in a clean room. The design of the microsystems consisted in two interdigitated platinum microelectrode arrays deposited on an insulating SiO_2 wafer (Fig. 1). Each array was composed of 50 microelectrodes measuring 100 μm wide and 9896 μm long. This microsystem geometry was chosen because it allowed for the measurement of conductivity changes between the 2 arrays and because it optimized the signal delivered. The objective was to electrodeposit PPy/sCoPc films both on the conductive microelectrode arrays and across the insulating gap separating the microelectrodes of the sensor.

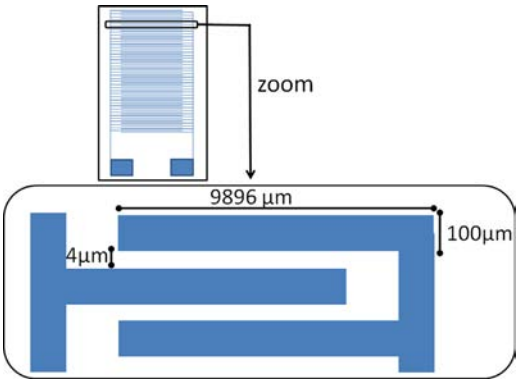

Fig. 1. Schematic drawing of the microsystem.

Consequently, the insulating gap between the neighboring electrodes had to be narrow enough, around 4 μm, to allow the PPy/sCoPc film to form a coating on the insulated gap and to electronically connect the two microelectrode arrays by polymer pathway.

The 4″ silicon wafers used in this study were 100-oriented, 500 μm thick, p-type doped and had a resistivity of 1 Ω cm^{-1} to 10 Ω cm^{-1}. They were thermally wet-oxidized, at 1200 °C in water vapour flux during 12 h to produce a 1.4 μm thick SiO_2 layer. In order to fabricate microsystems with this geometry, a Cr/Glass mask for lithography was designed using Cadence conception software, and it was fabricated using a Heidelberg DWL 250 optical pattern generator. Wafers and mask were pre-cleaned for 10 min in a mixture of H_2SO_4 (50 mL) and H_2O_2 (30 mL) to remove organic residues that contaminate their surface. Then, the wafer was dried under a N_2 stream and placed on a hot plate (Prazitherm) for 10 min at 120 °C. A layer of negative photoresist (AZ 5214, from Clariant) was spin-coated on the silicon wafer using a RC8-Karlsuss spin coater (30 s at a rotation speed of 3000 rpm). Wafer was again placed on the hot plate for 150 s at 120 °C before the photoresist was exposed, after alignment of the mask, to an UV radiation flux of 36 mJ cm^{-2} delivered by a double-sided EVG 620 aligner. After 2 min at 120 °C on the hot plate, the wafer was exposed, without the mask, to an additional UV dose of 210 mJ cm^{-2}. The last step of the photolithography process was the development of the wafer by immersion in AZ 726 developer for 1 min. The correct development of the resist and the appearance of the pattern were checked using an optical microscope before starting the deposition of metallic layers by sputtering to obtain conductive microelectrode arrays. Magnetron sputtering was done using a Plassys MP 500 system in a vacuum chamber pumped down to 3.10^{-6} mbar with primary rotating oil pump and secondary cryogenic CTI8 pump. The sputtering process started with an etching run (sputtering parameters: time: 1 min, pressure: 7.10^{-3} mbar with Ar gas, power: 250 W), followed by the deposition of a 30 nm adhesion layer of pure titanium (15 s at 1 A, 7.10^{-3} mbar with Ar gas, 150 W), and a 150 nm layer of pure platinum (1 min at 0.6 A, 7.10^{-3} mbar with Ar gas, 150 W). The dissolution of the remaining resist was finally done in acetone with ultrasonic waves, and the final microsystems composed of Ti/Pt microelectrodes arrays were controlled using an Olympus optical microscope.

2.2. Electrochemistry and surface analysis

Pyrrole was from ACROS (99% pure) and was distilled under reduced pressure before use. Lithium perchlorate was from Sigma Aldrich and used as electrolytic salt. A mixture of *n*-sulfonated cobalt phthalocyanines (sCoPc), known as $Co[(SO_3Na)_{2.3}Pc]$, was supplied by Europthal company as additive 8020 and used as molecular material. Some electrolytes were composed of 0.1 M pyrrole in an aqueous solution of 0.1 M $LiClO_4$. Other electrolytes were composed of pyrrole (0.1 M) and sulfonated cobalt phthalocyanine (0.05 M) with or without 0.5 M $LiClO_4$. These different electrolytes were electrochemically oxidized in order to deposit a thin solid film on array-patterned substrate. Electrochemical experiments were performed with a PGZ 100 potentiostat (Tacussel-Radiometer Analytical SA-France) controlled by the VoltaMaster 4 software. A standard three-electrode set-up was used to perform electrochemical experiments. A Saturated Calomel Electrode (SCE) and a platinum sheet were used as reference electrode and counter-electrode, respectively. The working electrode used was either a platinum wire for studying the electrochemical behaviour of the electrolytes or a Fluorine doped Tin Oxide (FTO) substrate (from Balzer, $R=120\ \Omega$, thickness: 2 mm) for surface analysis or both electrode arrays of microsystem to serve as gas sensor. All electrochemical experiments were carried out at room temperature (293 K).

The electrochemical oxidation of the electrolytes was performed by both potentiodynamic deposition using cyclic voltammetry technique and potentiostatic deposition using chronocoulometry technique.

The morphological features of all thin solid films were studied using a high-resolution Scanning Electron Microscope (SEM) and an Atomic Force Microscope (AFM). Once synthesized and dried, polymer films were examined, in a SEM Quanta 450 W from FEI, with an electron beam energy of 10 keV. These films were also studied, with a commercial AFM PicoSPM from Molecular Imaging. All AFM pictures were imaged using a commercial aluminium coated Si tip (mounted on 450 μm long single-beam cantilever with a resonance frequency of approximately 75 kHz and a spring constant of about 0.27 N m^{-1}). The scan rate was in the range of 2.40 Hz with a scanning density of 1024 lines per frame. The AFM was mounted on a floating table to achieve vibration insulation during investigations.

Polymer films were also characterized by X-ray Diffraction (XRD) Model D8 Advance Bruker, with Cu K_α radiation. The diffraction data were collected with a 0.01° step-width over a 2 theta range from 10 to 40°.

To examine the hydrophilicity of the polymer films, water contact angles were measured using a Dropscan contact angle analyzer (from Itconcept). The instrument is equipped with a CCD camera, a sample stage and a syringe holder. A 5 μL drop of ultrapure water was formed at the tip of a syringe needle and placed onto the polymer surface by raising the sample until a contact was made. Then, an image of the drop was captured, before contact angles were determined by drawing the tangent close to the edge of the droplet. For each sample at least 5 measurements were done at 3 different locations.

2.3. Gas chamber and gas measurements

The gas sensors, obtained from electrochemically polymer-modified microsystems, were put into in a Teflon gas chamber where they were exposed to dry synthetic air, used as carrier gas at a flow rate of 50 mL min^{-1}, until stabilization of the conductance value. For all sensors, the stabilization of the baseline was obtained after less than 30 min since air did not react with electrodeposited layers. At the end of the stabilization, ammonia was injected into the gas chamber (volume: 300 mL) and the conductance G of the sensors was measured as a function of time. The ammonia concentration was varied from 1 ppm to 100 ppm by dilution of ammonia, initially concentrated at 100 ppm, into synthetic air. For each concentration, the sensors were exposed for 5 min to ammonia used at a constant gas flow rate of 50 mL min^{-1}. Between each exposition to ammonia, the sensors were exposed to synthetic air during 1 h to allow desorption of ammonia molecules from the sensitive layers of the gas sensors. More details about this experimental set-up can be found in Ref. [18].

The responses of the sensors to ammonia were measured using Labview through a data acquisition system including a multi-channels input interfaced with a computer. The electrical potential U_r between the two microelectrode arrays of the sensors was recorded every 2 s using a divisor voltage bridge (at around 293 K). The conductance G of the sensors was deduced from these electrical measurements using Eq. (1):

$$G = \frac{U_r}{R(E-U_r)} \quad (1)$$

where $E=5$ V is the terminal voltage applied to the circuit and maintained constant during the experiments and R the adjusted resistance.

The limit of detection of the gas sensors was considered to be the minimum concentration necessary to obtain a signal which was at least three times more important that the background signal.

3. Results and discussion

3.1. Electrochemical deposition of thin films

3.1.1. Potentiodynamic electropolymerization of polypyrrole films

Polypyrrole was electrochemically synthesized for the first time by Diaz et al. [37]. This electropolymerization was performed at a platinum electrode from an electrolytic solution containing pyrrole, acetonitrile and lithium perchlorate. Further to these works, many studies have been dedicated to polypyrrole, and electrodeposition of polypyrrole is now well-controlled. The synthesis of polypyrrole can be achieved by potentiodynamic techniques such as cyclic voltammetry or by potentiostatic techniques such as chronoamperometry. It can also be performed on metallic or semi-conducting electrodes and in aqueous or organic solvents. The experimental parameters (applied potential, scan rate, nature and concentration of the dopant, …) used during the electrodeposition are also important since they can lead to polypyrrole films with very different chemical, electrical and structural properties [38,39].

In the present work, polypyrrole films were deposited on a platinum electrode by electrochemical oxidation from an aqueous solution of pyrrole and $LiClO_4$ both concentrated at 0.1 mol L^{-1}. During the anodic oxidation, the potential was swept from the open-circuit potential of the electrode (+0.1 V/SCE) to +1.5 V/SCE at a potential scan rate of 75 mV s^{-1} (Fig. 2a). An increase in the current density was observed from +0.7 V/SCE in the cyclic voltammogram (CV), and an oxidation peak can be observed at +1.0 V/SCE which is characteristic from the oxidation of pyrrole monomers into pyrrole radical cations. The oxidation of pyrrole was also observed during the next scans. This CV indicates that polypyrrole can be electrodeposited in potentiostatic mode if a potential of +1.0 V/SCE (or more) is applied. That is what we have done in a previous study where ammonia sensors based on polypyrrole films electrodeposited under many different conditions were tested to determine the influence of the salt nature, salt concentration, pyrrole concentration and electrodeposition potential on the sensors responses to ammonia [18]. In this work, the polymer film leading to the best results in terms of ammonia detection was electrodeposited at+2.0 V/SCE from an aqueous pyrrole and $LiClO_4$ solution. Taking into account these results, we will use, in the present study, polypyrrole films electrodeposited at +1 V/SCE (used as reference film) and +2 V/SCE for use as sensitive layers of ammonia gas sensors.

3.1.2. Potentiodynamic electropolymerization of polypyrrole/phthalocyanine films

In addition to standard polypyrrole films, it could be interesting to electrosynthesize hybrid materials made of polypyrrole matrix incorporating molecular compounds such as cobalt phthalocyanines. However, it is well-known that metal phthalocyanines are not soluble in polar solvents. In order to make them soluble, sulfonate groups have then been grafted onto the phthalocyanine ring forming sulfonated cobalt phthalocyanine (sCoPc). Therefore, aqueous electrolytic solutions containing pyrrole and sCoPc have been electro-oxidized from the free potential of the electrode (+0.075 V/SCE) to +1.5 V/SCE at a potential scan rate of 75 mV s^{-1}. The CV obtained from pyrrole and sCoPc has the same shape as the one obtained with pyrrole and lithium perchlorate even if two oxidation peaks can be observed at +0.8 V/SCE and +1.0 V/SCE during the first potential cycling. The additional oxidation peak could be due to the oxidation of the metal of the sulfonated phthalocyanine. During the following potential scans,

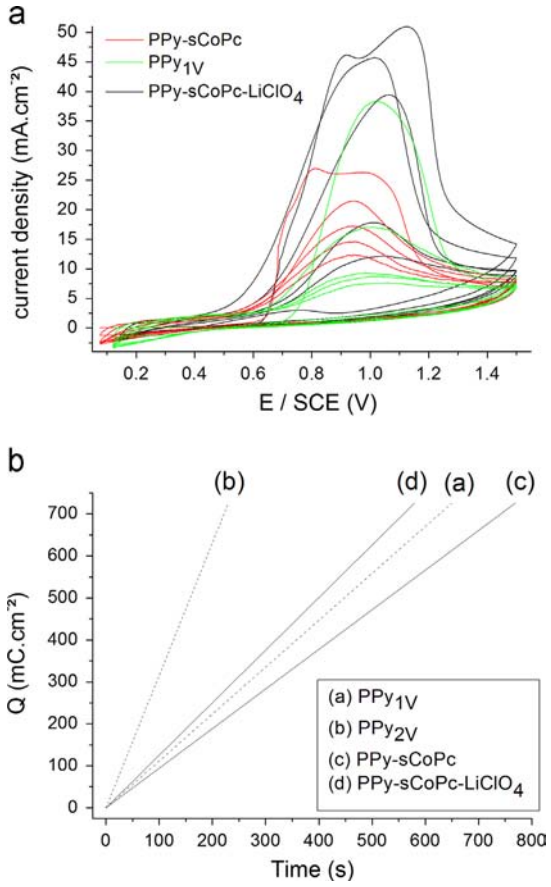

Fig. 2. Cyclic voltammetries (a) and chronocoulometries (b) obtained by electrochemical oxidation of aqueous solutions containing pyrrole+$LiClO_4$ or pyrrole+sCoPc or pyrrole+$LiClO_4$+sCoPc.

only the oxidation peak of the pyrrole is observed. The anodic electropolymerization of another electrolytic solution containing pyrrole, sCoPc and $LiClO_4$ was also performed. Resulting CV exhibited two peaks at +0.9 V/SCE and +1.1 V/SCE due to the electrochemical activity of cobalt in phthalocyanine and pyrrole oxidation, respectively. The CVs of Fig. 2 showed a higher current for Py–sCoPc–$LiClO_4$ than for Py–sCoPc electrolyte, thus indicating that the presence of lithium perchlorate facilitates charge carrier transport and then increases the oxidation reactions.

From the CVs obtained from Py–sCoPc and Py–sCoPc–$LiClO_4$ solutions, it can be deduced that the potentiostatic electrodeposition of hybrid materials can be achieved at a potential of +1.0 V/SCE.

3.1.3. *Potentiostatic electropolymerization of polypyrrole and polypyrrole/phthalocyanine films*

The electrochemical deposition of the sensitive layers of the ammonia gas sensors was achieved by potentiostatic technique rather than by potentiodynamic one because it allows a better control of the film thickness. More precisely, chronocoulometry was used in order to coat all platinum microelectrodes of the microsystem with a polypyrrole film of about 1.5 μm. This was done by applying an electrodeposition potential of +1.0 V/SCE between the microelectrode arrays used as working electrode and the reference electrode until reaching a total electric charge density of 730 mC cm^{-2} as calculated using Faraday's law [40,41]. After the completion of the electropolymerizations, a black film characteristic from polypyrrole was observed on the microelectrode surface in the absence of sCoPc in the electrolyte, and a dark blue film of PPy–sCoPc or PPy–sCoPc–$LiClO_4$ was observed after incorporation of sCoPc due to the mix between black PPy and blue sCoPc. The incorporation of the cobalt element in the polypyrrole matrix has also already been demonstrated using Glow Discharge Optical Emission Spectroscopy [36]. All resultant films adhered very strongly to the microelectrode surface as observed by visual inspection. As shown by the chronocoulometries given in Fig. 2b, the electric charge density of 730 mC cm^{-2} was reached after only 238 s for PPy film prepared at +2.0 V/SCE (denoted $PPy_{2\ V}$) when it was reached after 574 s and 737 s for PPy–sCoPc–$LiClO_4$ and PPy–sCoPc, respectively, and 653 s for PPy film prepared at +1 V/SCE ($PPy_{1\ V}$). Consequently, the kinetics of the polymer growth was strongly influenced by the composition of the electrolytic solution and the electrodeposition potential. More precisely, an increase of the electrodeposition potential, from +1.0 to +2.0 V/SCE, led to an increase of the kinetics. The presence of $LiClO_4$ also led to an increase of the kinetics, as can be observed by comparing the chronocoulometries of PPy–sCoPc–$LiClO_4$ and PPy–sCoPc.

3.2. *Characterization of the polymer films*

3.2.1. *Morphological features of the polymer films*

The morphological features of polypyrrole films and polypyrrole/phthalocyanine films were studied using scanning electron microscopy (SEM) and atomic force microscopy (AFM). This was done after electrodeposition on FTO substrates because it is easier to perform SEM and AFM microscopy on FTO rather than on microelectrodes and because the morphology is not affected by the nature of the substrate as it was confirmed by imaging some coatings deposited on both substrates. SEM images of polypyrrole films obtained at +1.0 V/SCE (Fig. 3a) and +2.0 V/SCE (not shown) were very similar. They exhibited a compact and globular structure with the formation of aggregates composed of tens of globules. The aggregate size varying from 5 μm to 20 μm. This globular structure is characteristic from polypyrrole films [42–44]. AFM picture (Fig. 3b) confirms the structure of PPy films since aggregates are clearly visible. The roughness of the PPy film appears to be very important since the biggest aggregates are 8 μm-high. On the contrary, the roughness of PPy–sCoPc films seems rather low as shown by AFM pictures (Fig. 3d). Furthermore, SEM microscopy reveals that the structure of the hybrid films is very homogeneous and composed of small submicrometric globules regularly distributed on the whole substrate (Fig. 3c). Only some rare aggregates are present on the polymer surface but the height of these aggregates does not excess 500 nm according to AFM pictures. The differences of morphology between polypyrrole and polypyrrole/phthalocyanine films probably result from the size and structure of the doping anion. When polypyrrole films are grown, perchlorate anions increase the conductivity of the electrolytic solution and play the role of dopants of the electrosynthesized polymer chain. When hybrid films are grown, sulfonate groups grafter on the cobalt phthalocyanine also plays the role of dopant of the polymer chain but their important size is not favourable to the easy growth of long polypyrrole chain. Consequently, it can be assumed that long polypyrole chains are obtained with perchlorate anions when short oligomers of polypyrrole are obtained in the presence of phthalocyanines. This leads to rougher films in the case of polypyrrole than in the case of polypyrrole/phthalocyanine.

The morphological features of PPy–sCoPc–$LiClO_4$ films are different from those of PPy and PPy–sCoPc films as can be observed in Fig. 3e and f. Indeed, AFM images indicate that the roughness is higher than that of PPy–sCoPc films, but smaller than the one of PPy since the biggest peaks of PPy–sCoPc–$LiClO_4$ are 3 μm-high. In these coatings, ClO_4^- and sulfonate groups grafted on phthalocyanines act concomitantly as doping agents, and the presence of $LiClO_4$ increases the conductivity of the electrolytic solution. Consequently, the electropolymerization process is easier than in the absence of

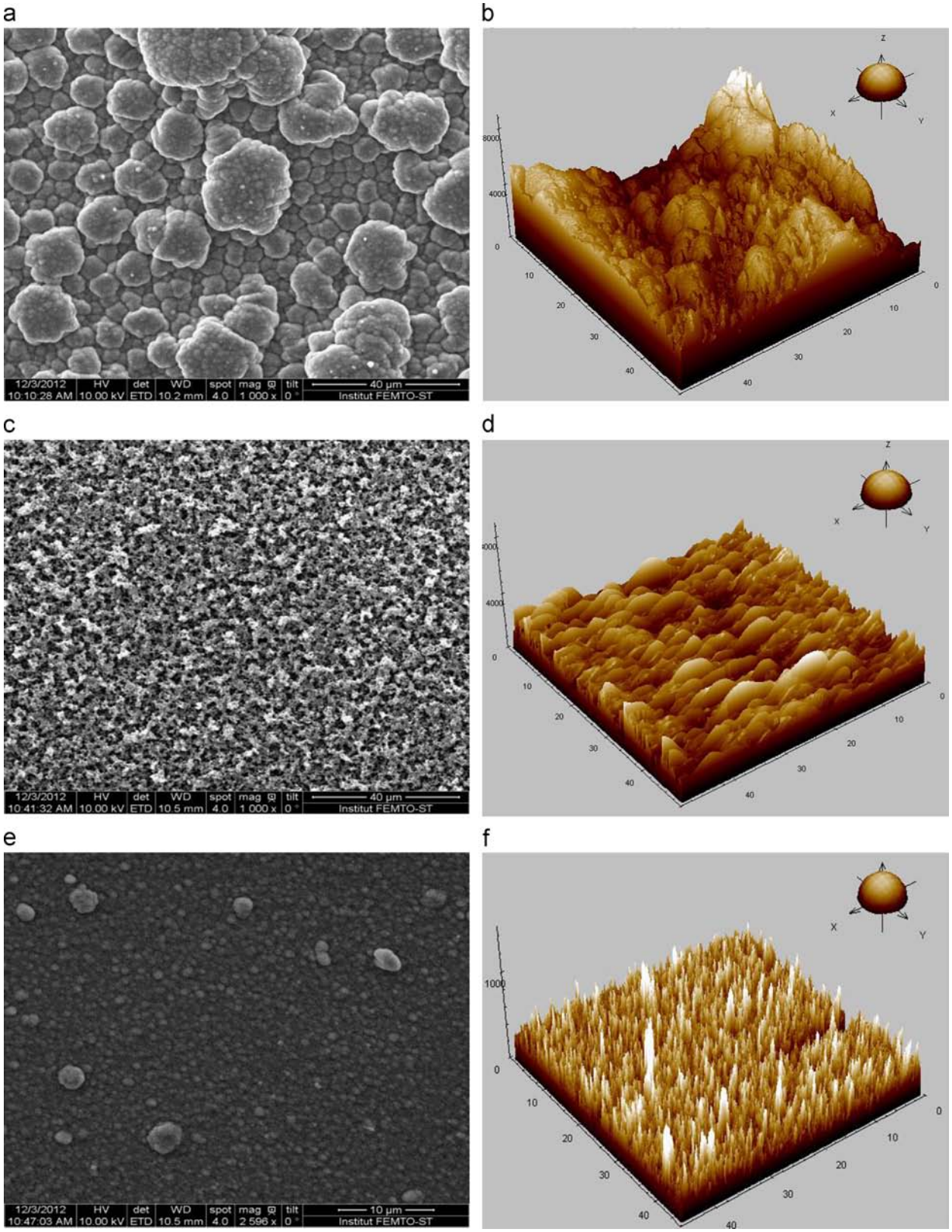

Fig. 3. SEM ((a), (c), (e)) and AFM ((b), (d), (f)) images of: $PPy_{1\ V}$ ((a), (b)), PPy/sCoPc/$LiClO_4$ ((c), (d)), PPy/sCoPc ((e), (f)) electrodeposited films grown on FTO substrates (magnification: × 1000).

$LiClO_4$ even if the phthalocyanines continue to limit the formation of long polypyrrole chains. The microstructure of PPy–sCoPc–$LiClO_4$ films is also very different from the globular structures previously described. Indeed, the microstructure is very homogeneous and presents an important porosity that was not observed for other polymer films.

3.2.2. XRD analysis of the polymer films

Fig. 4 shows the XRD patterns of $PPy_{1\ V}$, $PPy_{2\ V}$, PPy–sCoPc and PPy–sCoPc–$LiClO_4$ films electrodeposited on FTO substrates. $PPy_{1\ V}$ sample showed a single peak located at 26.5° (2θ) value which can be attributed to FTO substrates since the same peak was present in the XRD spectrum of naked FTO (not shown here). Consequently, polypyrrole films electrodeposited at +1.0 V/SCE were amorphous. On the contrary, several peaks are observed in XRD patterns of $PPy_{2\ V}$ that are not due to FTO substrate. These additional peaks are located at 13.5°, 15.5° and 19°. All these peaks have been attributed by considering the literature dedicated to XRD study of polypyrrole [45–51]. Thus, the peak located at 13.5° (2θ) value could be attributed to polypyrrole as well as the enhancement of the peak at 26.5° (2θ) value. However, polypyrrole must be considered as an amorphous material and the presence of peaks only indicates the partial crystalline nature of PPy electrodeposited at +2.0 V/SCE. In fact, this partial crystallinity comes from the presence of a rigid chain and localized structure even if the rigid benzene ring in the molecular chain prevents formation of a completely crystalline structure. The peak located at 19° (2θ) value was probably due to the crystalline perchlorate anions incorporated in the polypyrrole film and acting as dopants. The last peak at 15° (2θ) value could be attributed to protons bonded to nitrogen atoms of the polypyrrole chain as previously suggested by Cheah et al. [47]. It can also be noticed that the increase of the electrodeposition potential, from +1 V/ECS to +2 V/ECS, led to an increase of the crystallinity of the polymer film, probably because the film is more positively charged when electrodeposited at high potential. Consequently, more $LiClO_4$ counter-anions, favorable to the partial crystallization of the film, are incorporated in the polymer film at high electrodeposition potential.

Polymer hybrid films were also studied. PPy–sCoPc films exhibited only the peak characteristic from the FTO substrate and located at 26.5° 2θ value. So, the hybrid films are amorphous in the absence of lithium perchlorate. On the contrary, PPy–sCoPc–$LiClO_4$ films demonstrated some peaks at 13.5°, 15° and 19° 2θ values. The location of these peaks is similar to the location of the peaks observed for $PPy_{2\ V}$ films. Consequently the assignment of the peaks is the same: 13.5° 2θ value corresponds to polypyrrole chains, 15° 2θ value corresponds to protonated pyrrole units and 19° 2θ value corresponds to perchlorate anions doping polypyrrole. The high concentration of $LiClO_4$ (0.5 mol L^{-1}) in the electrolytic solution leading to PPy–sCoPc–$LiClO_4$ compared to the one used for the electrodeposition of $PPy_{1\ V}$ (0.1 mol L^{-1}) has probably favored the crystallization of some parts of the polymer chain. It can also be noticed that no peak attributable to sCoPc was observed on the XRD patterns of PPy–sCoPc and PPy–sCoPc–$LiClO_4$.

From these XRD patterns, it appears that a high electrodeposition potential and the presence of $LiClO_4$ at a high concentration are favorable to an increase of the crystallinity of the polymer films.

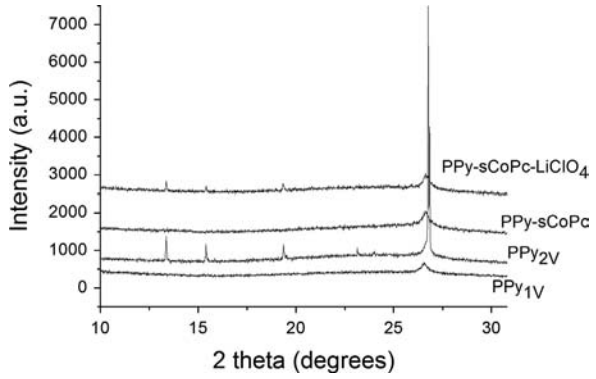

Fig. 4. XRD patterns of the different polymer films.

3.2.3. Wettability of the polymer films

The wettability of a polymer film, assessed from water contact angle measurements, of a polymer film is generally determined by the first 5–10 Å of the outermost layer [52,53]. This means that the wettability of any modified surface depends from various factors including the chemical composition of the electrodeposited polymer, the hydrophilicity of its functional groups, its roughness and its morphological features. So, the water contact angle was measured for each type of polymer film and the average values (obtained from 9 measurements) of the water contact angles were estimated. Polypyrrole films, doped by ClO_4^- anions, were the less hydrophilic polymer films since the average contact angle value was 71° ± 6°. For hybrid polypyrrole/phthalocyanine films electrodeposited in the absence of $LiClO_4$, the angle contact value was 0° indicating that these films were totally hydrophilic. So the presence of sulfonated cobalt phthalocyanines in the polymer films leads to an increase in the hydrophilicity of the films due to the presence of the grafted sulfonate groups that are well-known for their ability to enhance solubilization of compounds and to provide hydrophilic properties. Hybrid polypyrrole/phthalocyanine films doped by ClO_4^- anions had an average contact angle value of 37° ± 3°. This value seems to indicate that the presence of $LiClO_4$ into the hybrid films leads to a modification of the structure of the films rendering the sulfonyl groups more difficult to reach for the water molecules. This decreases the efficiency of the sulfonyl groups and so the resulting film is not fully hydrophilic.

3.3. Ammonia gas sensing properties of electrodeposited polymer films

In order to investigate the ammonia sensing properties of polypyrrole and polypyrrole/phthalocyanine polymer films, the conductance, response magnitude, response time and response reversibility of polymer-based sensors were studied.

The polymer-based sensors were exposed to synthetic air in the absence of ammonia until stabilization of the conductance of the sensors. The value of the conductance at the end of the stabilization process was denoted G_0. Once the stabilization achieved, the conductance G of the sensors was measured under exposition to ammonia diluted in synthetic air and used at different concentration in the range 1 ppm to 100 ppm. The exposure time was fixed to 300 s. After exposure, the sensor was kept in the gas chamber and exposed to synthetic air in the absence of ammonia to gain information about the reversibility of the sensor's response. From these measurements, the normalized conductance, given by G/G_0, was plotted as a function of time, as shown in Fig. 5. From this figure, it can be noticed that the normalized conductance decreased as soon as ammonia was injected in the gas chamber. On the contrary, the normalized conductance increased when the sensor was exposed to synthetic air after removing ammonia from the gas chamber. These trends were observed for the 4 polymer films and the results obtained are gathered in Table 1. More precisely, Table 1 gives the relative changes in the conductance $G_{\%}$ expressed as: $G_{\%} = 100 \times (G - G_0)/G_0$, and the measured slopes S of the curves giving the variation of G/G_0 with time.

The evolution of the conductance observed in Fig. 5 can be explained using previous works dedicated to the use of polypyrrole films as sensitive layers of ammonia gas sensors. Indeed, our group [18,54] and other groups [55,56] have already discussed and demonstrated the mechanism of interaction between polypyrrole films and ammonia molecules. In brief, polypyrrole is a p-type semi-conducting material made of both neutral and oxidized monomer units. When polypyrrole is exposed to ammonia gas, an electron transfer can occur between ammonia molecules and oxidized monomer units. More precisely ammonia acts as an electron donor that can give one electron from its free doublet to an oxidized monomer unit,

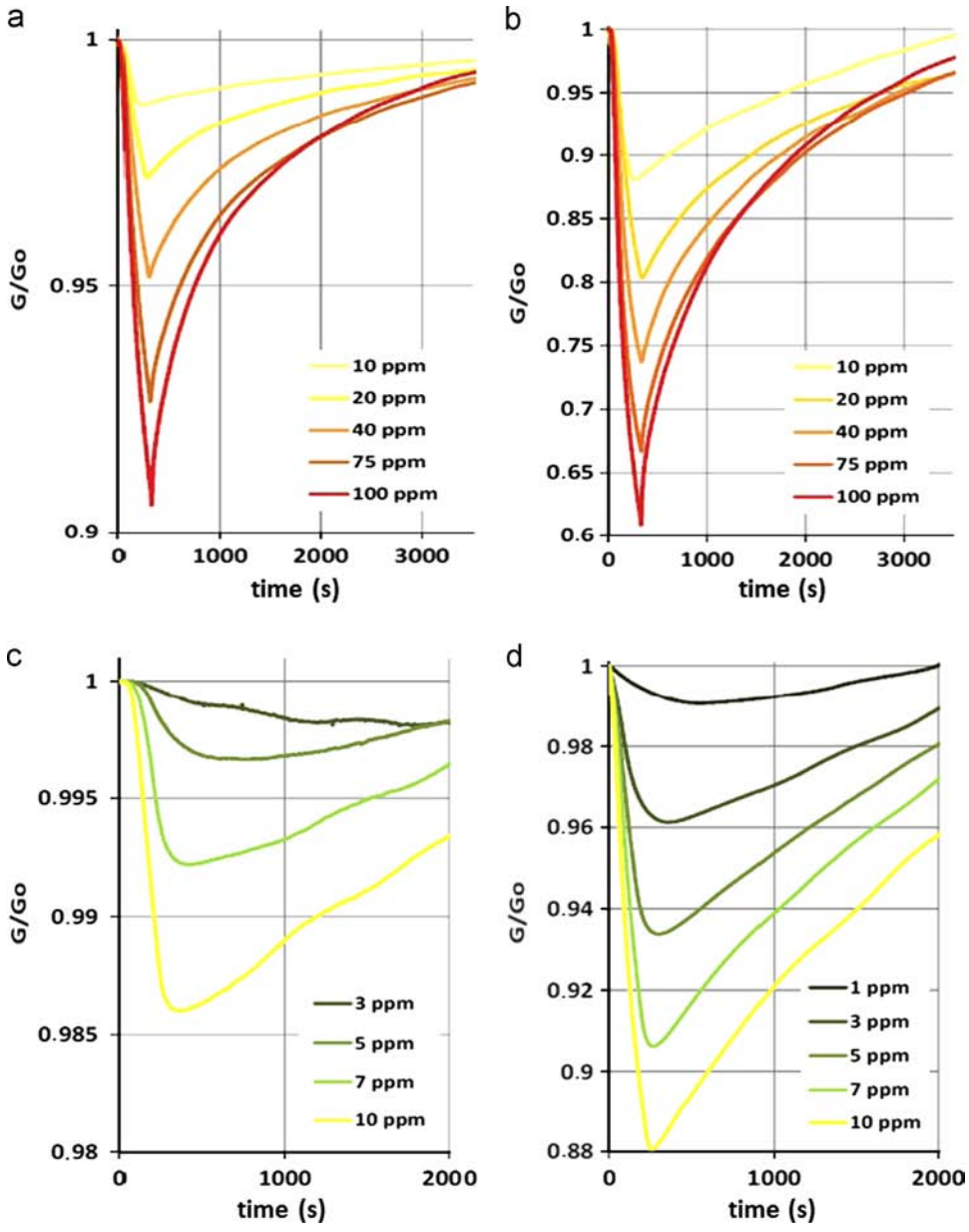

Fig. 5. Evolution of the normalized conductance of PPy–sCoPc ((a), (c)) and PPy–sCoPc–$LiClO_4$ ((b), (d)) films at high ((a), (b)) and low ((c), (d)) ammonia concentrations.

Table 1
Response of the sensors exposed to ammonia at different concentrations.

Polymer film	Parameter	[NH_3] (ppm)								
		1	3	5	7	10	20	40	75	100
$PPy_{1\ V}$	$G_{\%}$ (%)	No exploitable signal					2.0	3.8	6.8	10.7
	Slope (nS s^{-1})						130	153	311	495
$PPy_{2\ V}$	$G_{\%}$ (%)	0.2	0.8	1.8	3.6	5.9	9.5	16.0	22.8	28.3
	Slope (nS s^{-1})	7	52	98	216	286	416	614	1283	1773
PPy–sCoPc	$G_{\%}$ (%)	No exploitable signal		0.3	0.7	1.4	2.7	4.7	7.3	9.4
	Slope (nS s^{-1})			45	94	155	310	582	936	1237
PPy–sCoPc–$LiClO_4$	$G_{\%}$ (%)	0.5	3.5	6.4	9.2	11.8	18.9	25.5	33.7	38.3
	Slope (nS s^{-1})	57	322	560	821	1282	2082	3787	5626	6537

rendering immediately this monomer unit neutral. Consequently, the number of oxidized units in the polymer chain decreases during the adsorption of ammonia molecules (there is reduction of the polymer by ammonia gas) leading to a decrease of the conductance of the film, as observed in Fig. 5. On the contrary, the increase of the sensor's conductance observed after removal of ammonia gas and exposition

to synthetic air is due to the desorption of ammonia molecules from the polypyrrole film.

The mechanism of interaction between polypyrrole/phthalocyanine films and ammonia molecules has been less studied. However, phthalocyanines are semiconducting materials having many conjugated bonds, and the incorporation of such macrocycles into polymer chains of PPy generally results in the increase of the conjugation length and electron transfer [30]. It is known that metal phthalocyanines have highly conjugated π–π systems and two possible sites for gas adsorption: (i) the central metal ion and (ii) the conjugated π-electron system [57]. Consequently, we think that the interaction mechanism is similar to the one occurring between PPy and ammonia, ammonia acting as electron donor and the hybrid polymer films acting as p-material. The only difference is the adsorption of some ammonia molecules on the central cobalt that is expected to enhance the response of the hybrid materials-based sensors.

Polypyrrole electrodeposited at +1.0 V/SCE ($PPy_{1\ V}$) was used as reference sensor. As shown in Table 1, this sensor responded to ammonia concentration in the range from 20 ppm to 100 ppm. When exposed to ammonia concentrations lower than 20 ppm, the signal was not exploitable and so, the limit of detection of this sensor was 20 ppm. However, in the range from 20 ppm to 100 ppm, the relative changes in the conductance are not negligible since they vary from 2.0% (for 20 ppm of ammonia) to 10.7% (for 100 ppm). Similarly, for the same range, the slopes of the conductance—time responses increased from 130 nS s^{-1} to 495 nS s^{-1}. Gas sensors prepared from polypyrrole electrodeposited at +2.0 V/SCE ($PPy_{2\ V}$) exhibited more interesting characteristics for ammonia sensing. Indeed, they showed a better limit of detection that can be estimated to 3 ppm (the signal at 1 ppm is too low to be sure that it is not due to electrical interferences or background signal). They were also proved to be more sensitive to ammonia changes since the conductance increases from 0.8% (for 3 ppm of ammonia) to 28.3% (for 100 ppm). It must be noticed that such relative changes in the conductance are important as compared with the ones usually reported in the literature. The calculated slopes of the response of $PPy_{2\ V}$ were also more important that those obtained for $PPy_{1\ V}$ indicating that the response kinetics is faster in the case of $PPy_{2\ V}$.

Consequently, the improvement of the sensing characteristics is concomitant with the increase of the electrodeposition potential thus demonstrating that polypyrrole-based sensors are most sensitive when the polypyrrole film is electrosynthesized at high electrodeposition potential.

It was also noticed that the reversibility was good for both polypyrrole films obtained at +1.0 V/SCE and +2.0 V/SCE since the recovery of the initial response was about 75% and 85%, respectively, after 300 s whatever the ammonia concentration. To obtain a total reversibility, it would be necessary to heat the sensors to desorb quickly the ammonia molecules from the polymer films, or to use a longer desorption time.

The difference of behaviour between $PPy_{1\ V}$ and $PPy_{2\ V}$ can be explained by a higher conductivity or a higher crystallinity of the polypyrrole films electrodeposited at 2 V. Indeed, it is well accepted that electrochemical polymerization conditions, such as electrodeposition potential, affect properties such as crystallinity and conductivity of the polypyrrole [39,58,59]. It is reasonable to assume that the degree of crystallinity and conductivity affect the sensitivity of the material when it is employed in gas sensing applications. Considering the results obtained with PPy-based sensors and those reported in the literature [60], one can observe that a more crystalline nature positively impact on the availability of active sites for gas/polymer interaction, probably because the transfer of electron is easier in a crystalline structure than in an amorphous one.

Polypyrrole/phthalocyanine films electrodeposited with or whithout lithium perchlorate were also tested as sensitive layers for ammonia sensing. PPy–sCoPc-based sensors were sensitive to ammonia changes when the ammonia concentration was higher than 5 ppm (Fig. 5). The conductance varied from 0.3% (for 5 ppm of ammonia) to 9.4% (for 100 ppm), and the slopes of the responses increased from 45 nS s^{-1} to 1237 nS s^{-1}. The comparison between $PPy_{1\ V}$-based sensors and PPy–sCoPc-based sensors (both being electrodeposited at +1.0 V/SCE) indicates that PPy–sCoPc films led to a lower limit of detection (5 instead of 20 ppm), a faster kinetics (1237 nS s^{-1} instead of 495 nS s^{-1} at 1000 ppm) and a similar relative variation in the conductance (9.4% instead of 10.7% at 100 ppm). Consequently, using sCoPc instead of $LiClO_4$ in an aqueous pyrrole solution only resulted in a small improvement of the ammonia sensing abilities of the polymer films.

On the contrary, PPy–sCoPc–$LiClO_4$-based sensors exhibit very good abilities for ammonia sensing. First, it was possible to obtain an exploitable electrical signal for an ammonia concentration of only 1 ppm (Fig. 5d). This limit of detection is very low as compared to other tested sensors or to the literature. The relative changes in the conductance were also important since they varied from 0.5% (at 1 ppm) to 38.3% (at 100 ppm), thus proving that many ammonia molecules can adsorb on the hybrid polymer surface and be detected through conductance measurements. The slopes of their responses to ammonia changes were also particularly high (from 57 nS s^{-1} at 1 ppm to 6537 nS s^{-1} at 1000 ppm). Consequently, the presence of lithium perchlorate in the electrolytic solution led to an improvement of the sensing characteristics. Since it has been previously demonstrated that PPy–sCoPc–$LiClO_4$ films are partially crystalline when PPy–sCoPc films are amorphous, it seems that a higher crystallinity is favourable to the transfer of electron and charges inside the film, and thus, to en enhancement of the sensor response.

From these results, it can also be concluded that a better response is obtained thanks to the incorporation of sCoPc into the PPy (this is particularly true in the presence of $LiClO_4$). Since phthalocyanine is a semiconducting material having many conjugated bonds, the incorporation of this macrocycle into PPy chains is believed to increase the conjugation length and electron transfer in the polymer film [30]. Furthermore, the presence of two possible sites for gas adsorption in the phthalocyanine structure (the central metal ion and the conjugated π-electron system) in addition to the sites for gas adsorption already existing in the PPy structure can be responsible for the enhanced response of the polypyrrole/phthalocyanine films as compared to polypyrrole films.

The influence of the type of counter-ion on the crystallinity and conductivity of polypyrrole has been demonstrated by Li [60]. It is known that large organic counter-ions promote higher conductivity in PPy films, because they are more efficient space fillers and produce more isotropic polymers with higher crystallinity than those incorporating small inorganic species. The literature states that this more crystalline nature may positively impact on the availability of active sites for gas/polymer interaction. This is because PPy films comprising small inorganic ions or large organic ions have been demonstrated in the literature to have different conductivities and levels of crystallinity. Similarly, in this work, phthalocyanine can be considered as a large counter-ion that is incorporated in PPy films. Consequently, our results are in good agreement with the literature, which states that large organic counter-ions produce films with high crystallinity, resulting in high conductivity and improved sensing properties [60].

On the other hand, if the reversibility of PPy–sCoPc sensors was good with a conductance signal recovered at about 90%, the recovery, and so the reversibility, was far less satisfactory for PPy–sCoPc–$LiClO_4$ sensors. This may be due to a better adsorption of ammonia molecules on the polymer which renders desorption

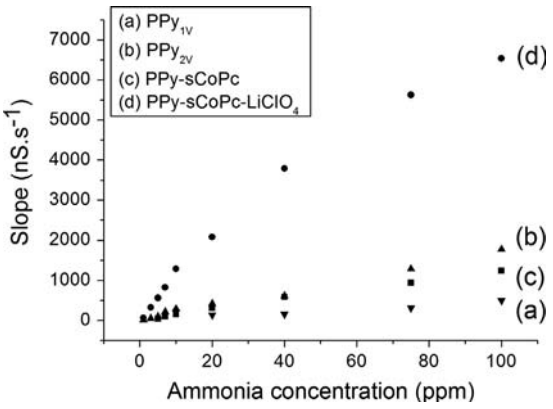

Fig. 6. Evolution of the slopes of gas sensor's electrical responses to ammonia concentrations.

of ammonia more difficult. However it must be noticed that the recovery rate obtained are high for a polymer-based sensor that operates at room temperature. Indeed it is very difficult to desorb at room temperature during the exposure to air all the ammonia molecules that are adsorbed in the polymer film during the exposure to ammonia as previously shown [54]. To obtain a better reversibility it would be probably necessary to heat the sensors to desorb the ammonia molecules from the polymer films. It could be also interesting to use a longer desorption time or to decrease exposure times. The repeatability of Py–sCoPc and Py–sCoPc–$LiClO_4$-based sensors was also tested by doing 5 sequences of exposure to ammonia and subsequent desorption at each ammonia concentration. The amplitude of the measured signal was constant after each exposure/desorption sequence whatever the ammonia concentration, thus proving the good repeatability of the response.

To compare more easily the conductance responses of the different polymer-based sensors, the evolution of the slopes as a function of the ammonia concentration was plotted in Fig. 6 (the slopes were deduced from the curves giving the evolution of the conductance with time at a given ammonia concentration). A linear relationship was observed between the slope and the ammonia concentration on the whole concentration range for $PPy_{1\,V}$, $PPy_{2\,V}$ and PPy–sCoPc sensors. On the contrary, the evolution of the PPy–sCoPc–$LiClO_4$ sensor can be divided into 2 parts: a first linear part for ammonia concentrations varying from 1 ppm to 10 ppm, followed by a less important increase of the slope from 10 ppm to 100 ppm that seems to indicate the beginning of the saturation of the adsorption sites. Fig. 6 also clearly indicates that the responses of PPy–sCoPc–$LiClO_4$ sensors are the best ones in terms of response amplitudes and sensitivities. Indeed, from Fig. 6, it is possible to estimate the sensitivity of each sensor (in nS s^{-1} ppm^{-1}). Thus, PPy–sCoPc–$LiClO_4$ is the most sensitive film with a sensitivity of 65.4 nS s^{-1} ppm^{-1} in the ammonia range from 1 ppm to 100 ppm when PPy–sCoPc, $PPy_{2\,V}$ and $PPy_{1\,V}$ exhibit a sensitivity of 12.4 nS s^{-1} ppm^{-1}, 17.7 nS s^{-1} ppm^{-1} and 4.9 nS s^{-1} ppm^{-1}, respectively.

Apart from this figure, other conclusions can be reached about these polymer-based gas sensors:

(i) the polymer-based gas sensors used in this work operate at room temperature. This is a strong advantage as compared to other chemiresistor sensors such as metallic oxides-based sensors working at high temperatures (from 300 °C to 500 °C) [61–64].

(ii) the polymer-based gas sensors used in this work present very competitive characteristics as compared to other ammonia gas sensors based on polymer films [56]. Indeed, the limit of detection is very low compared to ammonia gas sensors based on polypyrrole deposited through Langmuir–Blodgett technique (100 ppm) [65], or polypyrrole electrodeposited by Brie et al. (10 ppm) [66], or copolymers of polypyrrole and sulfonated polyaniline electrodeposited by Bai et al. (20 ppm) [67]. The amplitude of the signal is also more important that the one obtained in this work even if the comparison is difficult because of the different concentration ranges.

(iii) the main weakness of the polymer-based gas sensors used in this work is their selectivity. Indeed, ammonia is an electron-donor gas and it has been demonstrated that the reaction between polypyrrole or polypyrrole/phthalocyanine (which are p-type conducting materials) and ammonia leads to a strong decrease of the electrical conductance. However, this reaction is not specific from ammonia and the same reaction, leading to the same conductance decrease, should occur with most of the other electron-donor gases. On the contrary, many gases, in particular electron-acceptor gases, should not react with polypyrrole/phthalocyanine films. In this respect, the sensors are partially selective since they should not respond to volatile organic compounds (VOCs), or carbon oxides, for example.

4. Conclusion

In this paper, polypyrrole films and polypyrrole/phthalocyanine hybrid films were electrochemically synthesized on conductive substrates. Electron microscopy and atomic force microscopy were used to study the morphological features of the resulting films. It was shown that hybrid films were more homogeneous and had a less important roughness than granular polypyrrole films. The structure of the hybrid films electrodeposited from electrolytic solutions containing lithium perchlorate was also very different than the one synthesized in the absence of $LiClO_4$. The crystallinity of the films was analysed using X-ray diffraction and only the films obtained in the presence of $LiClO_4$ presented a partially crystalline structure. The hydrophilicity of the hybrid films was more important than that of polypyrrole films.

Then, both polypyrrole and polypyrrole/phthalocyanine films were electrodeposited on platinum interdigitated microelectrode arrays to obtain a microsystem that can be used as gas sensor, the polymer films acting as sensitive layer of the gas sensor. The conductance of the gas sensor was measured as a function of the ammonia concentration. Whenever polypyrrole-based sensors exhibited good responses to ammonia, the best responses were obtained for polypyrrole/phthalocyanine-based sensors. Indeed, the latter worked efficiently at room temperature with high detection efficiency, a good reversibility, a fast response, and a low detection limit (around 1 ppm). Consequently, we believe that these sensors have a great potential for environmental pollution monitoring since they were successfully tested in air and at ambient temperature. Furthermore, their detection limit is less than the ammonia toxicity values since the long-term allowed concentration that people may work in is 20 ppm [68]. From this work, it is expected that the usefulness of elaborating original hybrid materials combining electrodeposited polymer films with molecular compounds has been demonstrated, thus opening the way to new sensitive layers of gas sensors.

Acknowledgments

Tilia Patois was funded, through a PhD grant, by the Franche-Comté Regional Council. This work was also partly supported by the French RENATECH network and its FEMTO-ST technological facility.

References

[1] S. Shirakawa, E.J. Louis, A.G. MacDiarmid, C.K. Chiang, A.J. Heeger, J. Chem. Soc., Chem. Commun. (1977) 578.
[2] M. Braiek, H. Barhoumi, A. Maaref, N. Jaffrezic-Renault, Sensor Lett. 9 (2011) 2154–2157.
[3] B. Lakard, O. Segut, S. Lakard, G. Herlem, T. Gharbi, Sens. Actuators, B 122 (2007) 101–108.
[4] O. Segut, B. Lakard, G. Herlem, J.Y. Rauch, J.C. Jeannot, L. Robert, B. Fahys, Anal. Chim. Acta 597 (2007) 313–321.
[5] W. Prissanaroon-Ouajai, P.J. Pigram, R. Jones, A. Sirivat, Sens. Actuators, B 135 (2008) 366–374.
[6] R. Ansari, A.F. Delavar, A. Mohammad-Khah, J. Solid State Electrochem. 16 (2012) 3315–3322.
[7] A.R. Zanganeh, M.K. Amini, Electrochim. Acta 52 (2007) 3822–3830.
[8] M. Lin, X. Hu, Z. Ma, L. Chen, Anal. Chim. Acta 746 (2012) 63–69.
[9] X. Tu, Y. Gao, R. Yue, Q. Lu, Y. Zhou, Z. Lu, Anal. Methods 4 (2012) 4182–4186.
[10] J. Travas-Sejdic, H. Peng, P.A. Kilmaitin, M.B. Cannell, G.A. Bowmaker, R.P. Cooney, C. Soeller, Synth. Met. 152 (2005) 37–40.
[11] M.A. Booth, S. Harbison, J. Travas-Sejdic, Electroanalysis 24 (2012) 1311–1317.
[12] M.A. Booth, S. Harbison, J. Travas-Sejdic, Biosens. Bioelectron. 28 (2011) 362–367.
[13] G. Xu, S.B. Adeloju, Y. Wu, X. Zhang, Anal. Chim. Acta 755 (2012) 100–107.
[14] H. Jiang, A. Zhang, Y. Sun, X. Ru, D Ge, W. Shi, Electrochim. Acta 70 (2012) 278–285.
[15] D. Zane, G.B. Appetecchi, C. Bianchini, S. Passerini, A. Curulli, Electroanalysis 23 (2011) 1134–1141.
[16] M. Brie, R. Turcu, C. Neamtu, S. Pruneanu, Sens. Actuators, B 37 (1996) 119–122.
[17] L.H. Dall'Antonia, M.E. Vidotti, S.I. Cordoba de Torresi, R.M. Torresi, Electroanalysis 14 (2002) 1577–1586.
[18] T. Patois, J.B. Sanchez, F. Berger, J.Y. Rauch, P. Fievet, B. Lakard, Sens. Actuators, B 171–172 (2012) 431–439.
[19] H. Bai, O. Chen, C. Li, C. Lu, G. Shi, Polymer 48 (2007) 4015–4020.
[20] W.K. Jang, J. Yun, H.I. Kim, Y.S. Lee, Colloid. Polym. Sci. 291 (2012) 1–9.
[21] D.N. Huyen, N.T. Tung, T.D. Vinh, N.D. Thien, Sensors 12 (2012) 7965–7974.
[22] M.A. Chougule, S. Sen, V.B. Patil, Synth. Met. 162 (2012) 1598–1603.
[23] Y. Wu, S. Xing, J. Fu, J. Appl. Polym. Sci. 118 (2010) 3351–3356.
[24] D. Bouchta, N. Izaoumen, H. Zejli, M. El Kaoutit, K.R. Temsamani, Anal. Lett. 38 (2005) 1019–1036.
[25] N. Izaoumen, D. Bouchta, H. Zejli, M. El Kaoutit, A.M. Stalcup, K.R. Temsamani, Talanta 66 (2005) 111–117.
[26] C.C. Harley, A.D. Rooney, C.B. Breslin, Sens. Actuators, B 150 (2010) 498–504.
[27] F. Vilchez-Aguado, S. Gutierrez-Granados, S. Sucar-Succar, C. Bied-Charreton, F. Bedioui, New J. Chem. 21 (1997) 1009–1013.
[28] M.A. Carvalho de Medeiros, K. Gorgy, A. Deronzier, S. Cosnier, Mater. Sci. Eng., C 28 (2008) 731–738.
[29] U. Johanson, M. Marandi, V. Sammelselg, J. Tamm, J. Electroanal. Chem. 575 (2005) 267–273.
[30] S. Radhakrishnan, S.D. Deshpande, Mater. Lett. 48 (2001) 144–150.
[31] D.C. Tiwari, R. Sharma, K.D. Vyas, M. Boopathi, V.V. Singh, P. Pandey, Sens. Actuators, B 151 (2010) 256–264.
[32] B. Bott, S.C. Thorpe, Metal Phthalocyanine Gas Sensors, in: J.N.P.T. Moseley, D.E. Williams (Eds.), Techniques and Mechanisms in Gas Sensing, Adam Hilger, Bristol, 1991, p. 22.
[33] J.A. de Saja, M.L. Rodríguez-Méndez, Adv. Colloid Interface Sci. 116 (2005) 1–11.
[34] T. Sizun, M. Bouvet, Y. Chen, J.M. Suisse, G. Barochi, J. Rossignol, Sens. Actuators, B 159 (2011) 163–170.
[35] T. Sizun, M. Bouvet, J.M. Suisse, Talanta 97 (2012) 318–324.
[36] T. Sizun, T. Patois, M. Bouvet, B. Lakard, J. Mater. Chem. 22 (2012) 25246–25253.
[37] A.F. Diaz, K.K. Kanazawa, G.P. Gardini, J. Chem. Soc., Chem. Commun. (1979) 635–636.
[38] T. Patois, B. Lakard, S. Monney, X. Roizard, P. Fievet, Synth. Met. 161 (2011) 2498–2505.
[39] T. Patois, B. Lakard, N. Martin, P. Fievet, Synth. Met. 160 (2010) 2180–2185.
[40] N. Plesu, A. Kellenberger, M. Mihali, N. Vaszilcsin, J. Non-Cryst. Solids 356 (2010) 1081–1088.
[41] G.A. Snook, G.Z. Chen, J. Electroanal. Chem. 612 (2008) 140–146.
[42] M. Bazzaoui, J.I. Martins, E.A. Bazzaoui, L. Martins, E. Machnikova, Electrochim. Acta 52 (2007) 3568–3581.
[43] P.K. Sharma, G. Gupta, V.V. Singh, B.K. Tripathi, P. Pandey, M. Boopathi, B. Singh, R. Vijayaraghavan, Synth. Met. 160 (2010) 2631–2637.
[44] B. Lakard, L. Ploux, K. Anselme, F. Lallemand, S. Lakard, M. Nardin, J.Y. Hihn, Bioelectrochemistry 75 (2009) 148–157.
[45] C.O. Yoon, H.K. Sung, J.H. Kim, E. Barsoukov, J.H. Kim, H. Lee, Synth. Met. 99 (1999) 201–212.
[46] S. Chandra, S. Annapoorni, F. Singh, R.G. Sonkawade, J.M.S. Rana, R.C. Ramola, Nucl. Instrum. Methods Phys. Res., Sect. B 268 (2010) 62–66.
[47] K. Cheah, M. Forsyth, V.T. Truong, Synth. Met. 94 (1998) 215–219.
[48] Y. Nogami, J.P. Pouget, T. Ishiguro, Synth. Met. 62 (1994) 257–263.
[49] M.R. Warren, J.D. Madden, Synth. Met. 156 (2006) 724–730.
[50] R.Z. Pytel, E.L. Thomas, Y. Chen, I.W. Hunter, Polymer 49 (2008) 1338–1349.
[51] J.P. Wang, Y. Xu, J. Wang, X. Du, F. Xiao, J. Li, Synth. Met. 160 (2010) 1826–1831.
[52] E. Schrader, G.I. Loeb, Modern Approach to Wettability, Plenum Press, New York, 1992.
[53] K.L. Mittal, Contact Angle, Wettability and Adhesion, VSP, Utrecht, 1993.
[54] S. Carquigny, J.B. Sanchez, F. Berger, B. Lakard, F. Lallemand, Talanta 78 (2009) 199–206.
[55] I. Lähdesmäki, W.W. Kubiak, A. Lewenstam, A. Ivaska, Talanta 52 (2000) 269–275.
[56] H. Bai, G. Shi, Sensors 7 (2007) 267–307.
[57] T. Bosova, E. Koiltsov, A.K. Ray, A.K. Hassan, A.G. Gurek, V. Ahsen, Sens. Actuators, B 113 (2006) 127–134.
[58] Y. Osada, D.E. De Rossi, Polymer Sensors and Actuators, Springer, London, 2000.
[59] H. Masuda, D.K. Asano, Synth. Met. 135 (2003) 43–44.
[60] Y. Li, Synth. Met. 79 (1996) 225–227.
[61] A. Ponzoni, A. Depari, E. Comini, G. Faglia, A. Flammini, G. Sberveglieri, Sens. Actuators, B 175 (2012) 149–156.
[62] J. Sun, J. Xu, Y. Yu, P. Sun, F. Liu, G. Lu, Sens. Actuators, B 169 (2012) 291–296.
[63] T. Stoycheva, S. Vallejos, C. Blackman, S.J.A. Moniz, J. Calderer, X. Correig, Sens. Actuators, B 161 (2012) 406–413.
[64] J. Courbat, D. Briand, L. Yue, S. Raible, N.F. De Rooij, Sens. Actuators, B 161 (2012) 862–868.
[65] M. Penza, E. Milella, M.B. Alba, A. Quirini, L. Vasanelli, Sens. Actuators, B 40 (1997) 205–209.
[66] M. Brie, R. Turcu, C. Neamtu, S. Pruneanu, Sens. Actuators, B 37 (1996) 119–122.
[67] H. Bai, Q. Chen, C. Li, C. Lu, G. Shi, Polymer 48 (2007) 4015–4040.
[68] B. Timmer, W. Olthuis, A. Van den Berg, Sens. Actuators, B 107 (2005) 666–677.